

Single and double ionization of helium in heavy-ion impact

Imre Ferenc Barna¹, Károly Tókési^{1,2} and Joachim Burgdörfer¹

¹ Institute for Theoretical Physics, Vienna University of Technology, A-1040 Vienna, Austria

² Institute of Nuclear Research of the Hungarian Academy of Science (ATOMKI),
H-4001 Debrecen, PO Box 51, Hungary

Received 12 October 2004, in final form 9 February 2005

Published 22 March 2005

Online at stacks.iop.org/JPhysB/38/1001

Abstract

We present single- and double-ionization total cross sections for collisions of helium atoms with multiple charged ions. In our study we apply two different approaches, namely the *ab initio* coupled channel and the classical trajectory Monte Carlo (CTMC) method. We consider bare projectiles with charge states between two and eight with energies between 0.19 and 2.31 MeV/amu. We find that our coupled-channel calculations are very close to the experimental data even for the case when the Coulomb fields are strong. At the same time CTMC models, using different independent-particle approximations, show somewhat larger discrepancies compared to the experimental cross sections. We also present cross sections for 1.44 MeV/amu O^{q+} ($q = 4-7$) projectiles.

1. Introduction

One interesting and fundamental aspect of collision physics is the understanding of the ionization process. Differential spectra of ionized electrons provide detailed information about the dynamics of the ionization process. Characteristic structures in these spectra can be associated with different collision mechanisms. In recent decades both classical and quantum-mechanical theories have been extensively used to calculate the ionization cross sections of atoms and molecules for various projectiles. Single-ionization cross sections of atoms after impact of heavy-ion collisions are well understood, both experimentally and theoretically. However, accurate calculations for double-ionization cross sections, especially in the non-perturbative regime, where the electron–electron correlation plays a significant role, are still missing.

During the last two decades double ionization of helium atom in collisions with bare ions served as the primary test case. Knudsen *et al* [1] and Shah and Gilbody [2] employed coincidence techniques to measure charge-state resolved total cross sections. In the second part of the nineties Ullrich *et al* [3] realized kinematically complete experiments in which the individual momentum vectors of the two participating electrons could be resolved.

On the theoretical side, significant developments took place. Different *ab initio* methods were developed and used, mostly for proton–helium and antiproton–helium collisions. The forced impulse method (FIM) developed by Reading and Ford [4] presents one of the most successful method for proton– and antiproton–helium collisions. Time-dependent density functional theory [5] is another powerful method for describing non-perturbative many-electron ionization processes, even in the low keV/amu impact energy range. Keim *et al* [6] used density functional theory with a basis obtained from the basis generator method (BGM) to calculate ionization and electron transfer.

The independent-particle close-coupling methods in the semi-classical impact parameter treatment where the electron wavefunction is expanded either around the target or around target and projectile was successfully used by different authors to calculate ionization cross sections [7–9]. Very recently, a fully correlated, three-dimensional approach has been applied [10] to study the ionization of the He atom in antiproton collisions. The time-dependent Schrödinger equation is solved on a four-dimensional Cartesian lattice (LTDSE) and the ionization cross sections are determined using 75^4 lattice points. The *B*-spline basis for the construction of the active electron wavefunction was used by Sahoo *et al* [11]. *B*-splines have been widely used in atomic physics (see Martin [12]) because of their ability to represent the continuum channels more accurately in comparison to other conventional bases.

The aim of our paper is threefold. First, we present a detailed study of helium ionization by slow bare heavy ions as projectiles. The velocities of the projectile are chosen so that the Sommerfeld parameter $\eta = Z_p/v_p$ (Z_p is the charge and v_p is the velocity of the incident projectile) is close to the unity. The Sommerfeld parameter, η characterize the strength of Coulomb perturbation. When $\eta \gtrsim 0.5$ the perturbative models fail to describe the collision properties accurately. Except for the works by Pfeiffer *et al* [13] and Barna *et al* [14], to our knowledge, there are no other *ab initio* ionization calculations performed so far which consider heavier bare projectiles than He^{2+} . Secondly, we present coupled-channel (CC) calculations for ionization where the projectile carries electrons. In this case the projectile is described by the effective screened Coulomb potential. Thirdly, our results of the coupled-channel method, are compared with classical simulations of ionization which are readily performed, even for complex systems and thus a frequently employed tool. However their validity is questionable on two accounts; the lack of quantum effects beyond the ‘quantum’ binning of classical phase space for the initial and final state, and the neglect of electron–electron interaction beyond a mean-field independent-electron approximation. Helium is the only target for which a direct comparison between CTMC calculations and quantum calculations becomes possible.

In our previous work [14] the two-electron coupled-channel method was successfully used to calculate single- and double-ionization total cross sections for fast and highly charged ion collisions. The main idea of the method is the discretization of the electron continuum by Coulomb wave packets. The double-electron continuum is approximated by a large number of symmetrized products of single-particle Coulomb packets and includes a high degree of correlation. For $L = 0$ states we use *ss* + *pp* + *dd* angular correlated wavefunctions. Our *ab initio* method was also successfully used to calculate laser driven atomic processes in helium [15] and for positron–helium collisions [16].

In this work we apply two different classical trajectory Monte Carlo (CTMC) models. The CTMC method is an alternative classical theory to calculate the cross sections for the ejected electrons in A^{q+} and He collisions. Differences between the classical models result from different models for the underlying mean field by which the electron–electron interaction is taken into account. We refer to them as non-equivalent electron (NEE) CTMC [17] and equivalent electron (EE) CTMC models [18–21], respectively. While for the case of the non-equivalent electron model [17] the bare Coulomb interactions among the particles are used,

for the case of the equivalent electron approximation model potentials are considered. Both approaches are based on the numerical solution of the classical Hamilton equations of motions where all the particles participate in the collision process.

We organize the paper as follows: in section 2 we briefly outline our models. The results of our calculations are discussed and compared with experimental data in section 3. The paper ends with a short summary. Atomic units are used throughout the paper unless otherwise indicated.

2. Theory

2.1. The two-electron coupled-channel method

The coupled-channel (CC) method has been widely used in various fields of atomic collision physics with the recognition that it is one of the most reliable and powerful theoretical approaches. Our single-centre coupled-channel method has been introduced in detail in previous works [14, 22] and we give in the following only a brief summary. In the semi-classical approximation, the projectile moves on a straight-line trajectory, with constant velocity v and impact parameter b . The projectiles are considered to be classical point charges without inner structure.

To study the ionization process we solve the time-dependent Schrödinger equation with a time-dependent external Coulomb field

$$i \frac{\partial}{\partial t} \Psi(\mathbf{r}_1, \mathbf{r}_2, t) = (\hat{H}_{\text{He}} + \hat{V}(t)) \Psi(\mathbf{r}_1, \mathbf{r}_2, t), \quad (1)$$

where \hat{H}_{He} is the Hamiltonian of the unperturbed helium atom

$$\hat{H}_{\text{He}} = \frac{p_1^2}{2} + \frac{p_2^2}{2} - \frac{2}{r_1} - \frac{2}{r_2} + \frac{1}{|\mathbf{r}_1 - \mathbf{r}_2|} \quad (2)$$

and $\hat{V}(t)$ is the projectile–electron interaction

$$\hat{V}(t) = -Z_p \left(\frac{1}{R_1(t)} + \frac{1}{R_2(t)} \right) \quad (3)$$

with $R_i(t) = ((x_i - b)^2 + y_i^2 + (z_i - v_p t)^2)^{1/2}$, $i = 1, 2$ for bare projectiles. For projectiles carrying electrons we employ time-dependent independent-particle model potentials to be discussed below. To solve equation (1) we expand $\Psi(\mathbf{r}_1, \mathbf{r}_2)$ in the basis of eigenfunctions $\{\Phi_j\}$ of the time-independent Schrödinger equation

$$\hat{H}_{\text{He}} \Phi_j(\mathbf{r}_1, \mathbf{r}_2) = E_j \Phi_j(\mathbf{r}_1, \mathbf{r}_2), \quad (4)$$

where

$$\Psi(\mathbf{r}_1, \mathbf{r}_2, t) = \sum_{j=1}^N a_j(t) \Phi_j(\mathbf{r}_1, \mathbf{r}_2) e^{-iE_j t}, \quad (5)$$

and $a_j(t)$ are the time-dependent expansion coefficients for the various channels described by the wavefunctions Φ_j . Inserting this ansatz into equation (1) leads to a system of first-order differential equations for the expansion coefficients

$$\frac{da_k(t)}{dt} = -i \sum_{j=1}^N V_{kj}(t) a_j(t) e^{i(E_k - E_j)t}, \quad (k = 1, \dots, N), \quad (6)$$

where V_{kj} is the coupling matrix $\langle \Phi_k(\mathbf{r}_1, \mathbf{r}_2) | \hat{V}(t) | \Phi_j(\mathbf{r}_1, \mathbf{r}_2) \rangle$ including the symmetrized products of the projectile–electron single-particle interaction matrix elements and electron–electron single-particle overlap matrix elements, respectively.

Denoting the ground state with $k = 1$, we use the following initial conditions for solving (6):

$$a_k(t \rightarrow -\infty) = \begin{cases} 1 & k = 1 \\ 0 & k \neq 1. \end{cases} \quad (7)$$

The total cross section for occupying the helium eigenstate k can be calculated as

$$\sigma_k = \int P_k(\mathbf{b}, t \rightarrow \infty) d^2b \quad (8)$$

with the probability

$$P_k(\mathbf{b}, t \rightarrow \infty) = |a_k(t \rightarrow \infty)|^2. \quad (9)$$

The coupled system of equation (6) is solved numerically by using a Runge–Kutta–Fehlberg method of fifth order with embedded automatical time step regulation. The conservation of the norm of the wavefunction is fulfilled better than 10^{-8} during the collision.

The eigenfunctions Φ_j in equation (4) are obtained by diagonalizing the Hamiltonian in a basis of orthogonal symmetrized two-particle functions f_μ so that

$$\Phi_j(\mathbf{r}_1, \mathbf{r}_2) = \sum_{\mu} b_{\mu}^{[j]} f_{\mu}(\mathbf{r}_1, \mathbf{r}_2). \quad (10)$$

For the single-particle wavefunctions we use an angular momentum representation with spherical harmonics $Y_{l,m}$, hydrogen-like radial Slater functions and radial regular Coulomb wave packets. The Slater function reads

$$S_{n,l,m,\kappa}(\mathbf{r}) = c(n, \kappa) r^{n-1} e^{-\kappa r} Y_{l,m}(\theta, \varphi), \quad (11)$$

where $c(n, \kappa)$ is the normalization constant. A regular Coulomb wave packet

$$C_{k,l,m,Z}(\mathbf{r}) = q(k, \Delta k) Y_{l,m}(\theta, \varphi) \int_{E_k - \Delta E_k/2}^{E_k + \Delta E_k/2} F_{k,l,Z}(r) dk \quad (12)$$

with normalization constant $q(k, \Delta k)$ is constructed from the radial Coulomb function

$$F_{k,l,Z}(r) = \sqrt{\frac{2k}{\pi}} e^{\frac{\pi\eta}{2}} \frac{(2\rho)^l}{(2l+1)!} e^{-i\rho} |\Gamma(l+1-i\eta)| {}_1F_1(1+l+i\eta, 2l+2, 2i\rho), \quad (13)$$

where $\eta = Z/k$, $\rho = kr$.

The wave packets cover a small energy interval ΔE_k and thereby form a discrete representation of the continuum which can be incorporated into our finite basis set. The normalized Coulomb wave packets are calculated up to 315 au radial distance or more to achieve a deviation of less than 1% from unity in their norm.

In our approach two different effective charges Z entering the wavefunction have been used to take into account the difference between the singly and the doubly ionized electrons. For singly ionized states we have used $Z = 0.95$ and for the doubly ionized case $Z = 1.9$, respectively. We cover the single and double continuum up to 6 au energy equidistantly.

Out of the single-particle states (11), (12) we have used 17 s-functions (nine Slater functions (SF), four wave packets (WP) with $Z = 0.95$ and four WP with $Z = 1.9$), 18 p-functions (six SF, six WP with $Z = 0.95$ and six WP with $Z = 1.9$) and 12 d-functions (four SF, four WP with $Z = 0.95$ and four WP $Z = 1.9$) to construct the symmetrized basis functions $f_{\mu}(\mathbf{r}_1, \mathbf{r}_2)$. For the $L = 0$ configurations we have used ss + pp + dd wavefunctions to

get a ground state energy of -2.901 au which is reasonably accurate compared to the ‘exact’ value of -2.903 au. For the $L = 1, 2$ states we have used sp or sd configurations.

The diagonalization process gives us 465 basis states which correspond to 1490 different collision channels including different m_l sub-states. Our highest energy eigenvalue is at 27.8 au. In order to test for convergence of expansion (5) we have tried different basis sets. Our results demonstrate that the channels with energies above 5 au contribute very little to the ionization probabilities. Between the first ionization threshold (-2.0 au) and the lowest auto-ionizing quasi-bound state ($‘2s2s’ E = -0.77$ au $L = 0$) our basis contains 22 discretize continuum states per L providing the major contribution for single ionization.

In order to separate excitation, double- and single-ionization cross sections from each other we use a Feshbach projection [14] and complex scaling. In the first step we construct a new ‘reference’ Hilbert subspace which is split into three different orthogonal subspaces characterized by the properties of the two electrons: (1) bound–bound, (2) bound–ionized and (3) ionized–ionized electrons, respectively. In the second step we project our ‘calculation’ Hilbert subspace onto the reference space and determine the excitation, single- and double-ionization contributions. The decomposition into different ionization contributions depends on the parameters of the continuum wavefunctions, e.g. the effective charge of the Coulomb functions used which can modify our results up to 8%. To fix the effective charge of the Coulomb wavefunction used for our helium wavefunctions we compare the excitation and single-ionization cross sections with the results obtained from the complex scaling [15]. Doubly excited states embedded in the continuum (e.g. ‘ $2s2s$ ’ while this labelling should not be taken literally because of the strong electron–electron correlation [23]) can be identified by the method of complex scaling and therefore the double-excitation and the single-ionization states can be separated. This new combination of the two methods is still not rigorously exact but is much better than the Feshbach method alone and reduces the ambiguity.

2.2. Classical trajectory Monte Carlo approximations

In both versions of the present CTMC approach, Newton’s classical non-relativistic equations of motion are solved numerically for a large number of trajectories for given initial conditions. The equations of motion were integrated using a standard Runge–Kutta method.

2.2.1. Non-equivalent electron CTMC model (NEE-CTMC). The four structureless particles are characterized by their masses and charges. The forces acting among the four bodies are taken to be pure Coulombic. The interaction between the two active electrons of the helium atom is, however neglected during the collision. The two electrons are treated as non-equivalent. They are represented by micro-canonical ensembles with energies corresponding to the first and second ionization potentials, respectively. We note that this type of CTMC model is the classical analogue of the quantum-mechanical treatment of He atom when the two-electron wavefunction is built as a product of the two different single-particle wavefunctions. Each wavefunction satisfies the time-dependent Schrödinger equation with different model potentials (or with effective charges) [24].

In our model the binding energies of the electrons in the He atom are chosen conveniently [25] as 2 au for the inner electron and 0.903 au for the outer electron, respectively. The impact parameter of the projectile as well as the positions and the velocities of the electrons moving in the field of the target nucleus is randomly selected. To distinguish between the various final states, the exit channels are identified at large distances from the collision center. The total cross section for a specific event i is calculated from

$$\sigma_i = \frac{\pi N_i b_{\max}^2}{N}. \quad (14)$$

The statistical uncertainty for a cross section is given by

$$\Delta\sigma_i = \sigma_i \left(\frac{N - N_i}{NN_i} \right)^{1/2}. \quad (15)$$

In (14), (15), N is the total number of trajectories calculated for the impact parameters less than b_{\max} , N_i is the number of trajectories that satisfy the criteria for the process under consideration and b_i is the actual impact parameter for the event i specified by a set of collision product criteria.

2.2.2. Equivalent electron CTMC model (EE-CTMC). In this model three particles are explicitly treated, the projectile, the active atomic electron (e) and the remaining helium ion (He^+). The interaction between the active target electron and the projectile is purely Coulombic. For the description of the interaction between the projectile and the helium core, and between the active electron and the helium core a model potential is used which is based on Hartree–Fock calculations [26]:

$$V(r) = -[(Z - 1)\Omega(r) + 1]/r, \quad (16)$$

where Z is the nuclear charge and

$$\Omega(r) = [Hd(e^{r/d} - 1) + 1]^{-1}. \quad (17)$$

Using energy minimization, Garvey *et al* [27] obtained the following parameters $H = 1.77$ au and $d = 0.381$ au for He. We note that this type of CTMC model is the classical analogue of the quantum-mechanical model in which the time-dependent two-electron wavefunction is built as a product of two identical single-particle wavefunctions [24]. The initial conditions of an individual collision are chosen at sufficiently large internuclear separation from the collision center, where the interactions among the particles are negligible. These initial conditions are selected as described by Reinhold and Falcón [28] for non-Coulombic systems. A micro-canonical ensemble characterizes the initial state of the target. The initial conditions were taken from this ensemble, which is constrained to an initial binding energy of He(1s), 0.903, au. The three-dimensional CTMC calculation is performed as described by Olson and Salop [19]. From the trajectory calculations we obtain the one-electron ionization probabilities as a function of the impact parameter b as

$$P_i(b) = \frac{N_i(b, \Delta b)}{N\Delta b}, \quad (18)$$

where $N_i(b, \Delta b)$ is the number of trajectories at the impact parameter range between $b - \Delta b/2$ and $b + \Delta b/2$ satisfying the criteria of the ionization. The single-ionization cross section of He can be calculated as

$$\sigma_i^+ = 2\pi \int_0^\infty b P_i^+(b) db, \quad (19)$$

where $P_i^+(b) = 2P_i(b)$. In the independent-particle approach the double-ionization cross section of He can be written as

$$\sigma_i^{++} = 2\pi \int_0^\infty b P_i^{++}(b) db, \quad (20)$$

where $P_i^{++}(b) = P_i^2(b)$.

Table 1. Total single-ionization cross sections; comparison of experimental data with the non-equivalent (NEE) and the equivalent electron (EE) CTMC model calculations, and coupled-channel (CC) calculations, respectively. The statistical CTMC errors are less than 1.5%. All cross sections are in units of 10^{-16} cm².

Proj.	Energy (MeV/amu)	Z/v (amu)	Exp. value σ^+	EE-CTMC		
				NEE-CTMC	Garvey	CC
He ²⁺	0.63	0.40	1.13 ± <8%	0.63	0.958	1.08
"	1.44	0.26	0.62 ± <5%	0.303	0.474	0.61
"	2.31	0.20	0.44 ± <5%	0.191	0.319	0.42
Li ³⁺	0.64	0.59	2.5 ± <8%	1.26	1.936	2.42
"	1.44	0.4	1.38 ± <5%	0.65	1.03	1.35
"	2.31	0.3	0.98 ± <5%	0.42	0.650	0.95
B ⁵⁺	0.19	1.81	7.4 ± <8%	5.3	4.91	4.9
"	0.64	0.98	5.1 ± <8%	2.9	4.44	4.7
"	1.44	0.65	3.4 ± <8%	1.56	2.54	3.32
"	2.31	0.51	2.44 ± <8%	1.01	1.68	2.2
C ⁶⁺	0.64	1.18	6.0 ± <8%	3.87	5.97	5.2
"	1.44	0.78	4.5 ± <8%	2.09	3.46	4.3
"	2.31	0.62	3.3 ± <8%	1.41	2.45	3.1
O ⁸⁺	0.64	1.57	7.9 ± <8%	1.6	8.94	6.1
"	1.44	1.04	6.7 ± <8%	3.33	5.662	5.8
"	2.26	0.83	5.4 ± <5%	2.24	3.994	5.1

3. Results

In the following we consider the bare projectiles He²⁺, Li³⁺, B⁵⁺, C⁶⁺ and O⁸⁺ as projectiles with impact energies 0.19-2.31 MeV/amu. The corresponding experimental data can be found in [1].

Tables 1 and 2 show the measured single- and double-ionization total cross sections, respectively, together with the results of our coupled-channel and CTMC calculations. The ratios between the double- to single-ionization total cross sections are listed in table 3. The third column of the tables shows the Sommerfeld parameter $\eta = Z_p/v_p$. This parameter measures the strength of the projectile field. For $\eta \gtrsim 0.5$, perturbation theory is expected to break down.

For single-ionization cross sections the coupled-channel method gives better agreement with experiments than the CTMC methods. As an exception we mention the 0.64 MeV/amu data for O⁸⁺ projectiles where the independent-electron CTMC result is closer to experimental data than the CC. We found that the equivalent electron CTMC results are typically closer to the experimental cross sections than the non-equivalent electron CTMC. This is not surprising as the NEE model underestimates the multiplicity of the available electrons relatively easily ionized by an energy transfer of the order of the first ionization potential. Even for Sommerfeld parameters larger than unity our coupled-channel results are in good agreement with experimental data. To achieve such correspondence we used 1245 channels for systems where the Sommerfeld parameter is larger than unity. For collision systems with $0.5 \leq \eta \leq 1$ we used an intermediate number of channels (525) to get our recent results. In systems with $\eta < 0.5$, 'only' 340 channels were used. In all calculations the channels above 10 au energy were completely neglected. Our experience clearly shows that in order to obtain the converged results a particular choice of an optimized basis set for each collision system is required. As a

Table 2. Double-ionization total cross sections; comparison of experiments with two different (NEE and EE) CTMC model calculations, and coupled-channel calculations, respectively. The CTMC errors are less than 5%. All cross sections are in units of 10^{-16} cm².

Proj.	Energy (MeV/amu)	Z/v (amu)	Exp. value σ^{++}	NEE-CTMC	EE-CTMC Garvey	CC
He ²⁺	0.63	0.40	0.0160 ± <10%	0.0396	0.099	0.0158
"	1.44	0.26	0.0035 ± <11%	0.01193	0.0347	0.0031
"	2.31	0.20	0.0022 ± <10%	0.0046	0.019	0.0018
Li ³⁺	0.64	0.59	0.074 ± <11%	0.143	0.287	0.069
"	1.44	0.4	0.018 ± <10%	0.041	0.107	0.014
"	2.31	0.3	0.0085 ± <10%	0.0203	0.0552	0.0081
B ⁵⁺	0.19	1.81	1.76 ± <11%	0.32	0.543	1.0
"	0.64	0.98	0.41 ± <11%	0.56	0.812	0.32
"	1.44	0.65	0.113 ± <8%	0.19	0.409	0.08
"	2.31	0.51	0.059 ± <11%	0.105	0.231	0.048
C ⁶⁺	0.64	1.18	0.59 ± <11%	0.923	1.29	0.48
"	1.44	0.78	0.182 ± <11%	0.345	0.551	0.12
"	2.31	0.62	0.092 ± <11%	0.175	0.366	0.080
O ⁸⁺	0.64	1.57	1.32 ± <8%	0.602	1.868	0.9
"	1.44	1.04	0.45 ± <8%	0.775	1.008	0.3
"	2.28	0.83	0.31 ± <5%	0.405	0.707	0.23

Table 3. The ratio $R = \sigma^{++}/\sigma^{+}$ obtained from the cross sections of table 1 and 2. All data should be multiplied by 10^{-3} , experimental accuracy is about 9%.

Proj.	Energy (MeV/amu)	Z/v (amu)	Exp. value	NEE-CTMC	EE-CTMC Garvey	CC
He ²⁺	0.63	0.40	14	63	103	15
"	1.44	0.26	5.7	39	73	5.1
"	2.31	0.20	5	24	58	4
Li ³⁺	0.64	0.59	30	113	148	28.5
"	1.44	0.4	13	63	103	10
"	2.31	0.3	8.6	48	85	8.5
B ⁵⁺	0.19	1.81	237	60	110	204
"	0.64	0.98	80	193	182	68
"	1.44	0.65	33	121	161	24
"	2.31	0.51	24	104	137	22
C ⁶⁺	0.64	1.18	98	238	216	92
"	1.44	0.78	41	165	159	28
"	2.31	0.62	28	124	149	26
O ⁸⁺	0.64	1.57	166	376	208	150
"	1.44	1.04	67	232	178	51
"	2.26	0.83	57	180	177	45

pragmatic solution to find an optimized basis we always start with the first Born approximation including all channels. The distribution and the number of the significantly populated channels gives us a first-order guess as to what a convergent basis set should look like. The three different numbers of states presented above have proven to be a practical solution.

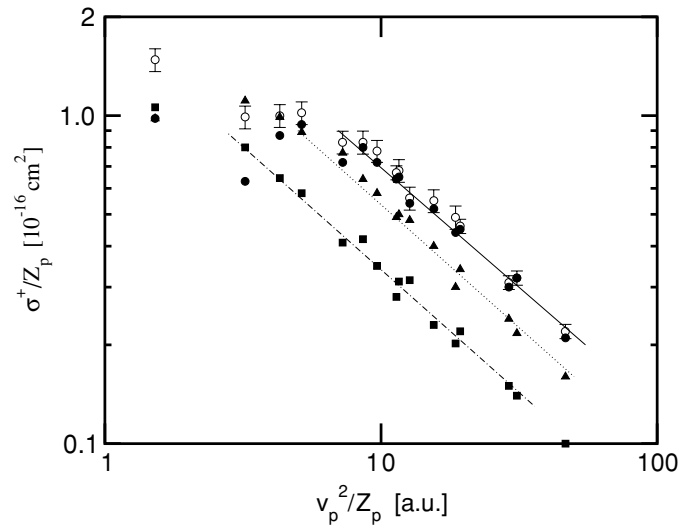


Figure 1. Scaled single-ionization cross sections from table 1. Open circles: experimental results [1], full circles: CC, full triangles: EE-CTMC, full squares: NEE-CTMC. The curve through the data is drawn to guide the eyes.

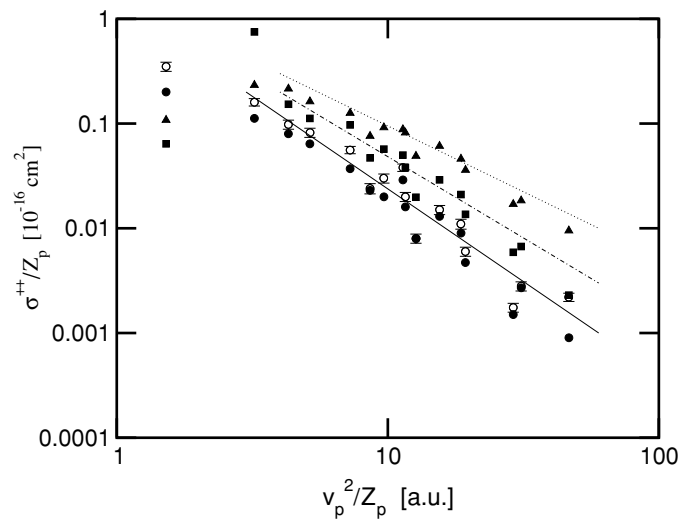


Figure 2. Scaled double-ionization cross sections from table 2. Notation is the same as in figure 1.

For the case of double ionization, the coupled-channel method gives in most cases better results than the CTMC model. Thanks to the large number of the double-ionized channels, even for strong perturbation the results agree well with experimental data. In contrast to the case of the single ionization, here the results of NEE-CTMC model are closer to the experimental than the results of EE-CTMC. The reason is most likely that in the non-equivalent electron approximation the binding energies of the two electrons in the atom can be independently specified according to the first and second ionization threshold. To visualize the differences between the EE-CTMC and NEE-CTMC models, we show in figures 1 and 2 the scaled

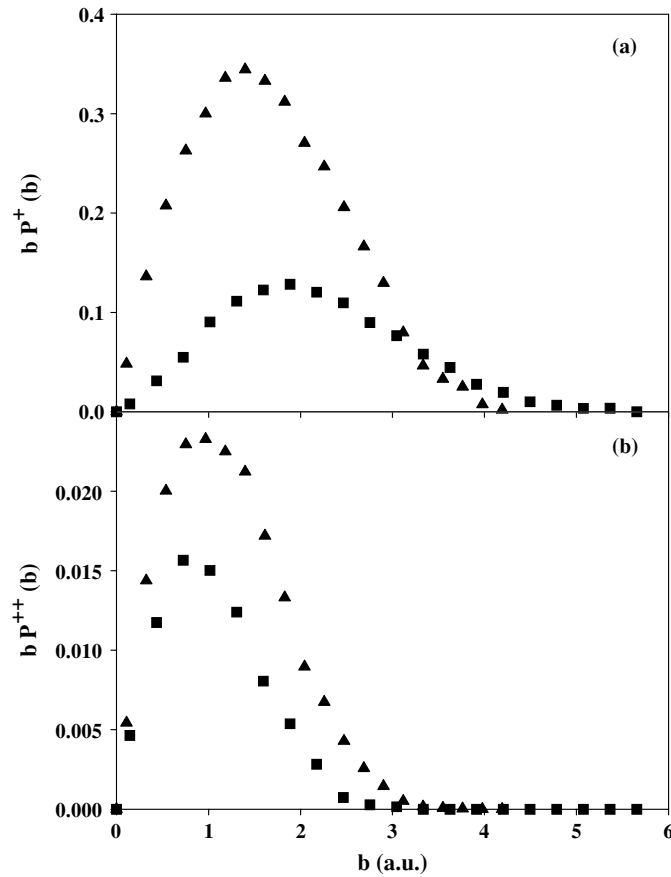


Figure 3. Impact parameter dependence of the single- (panel (a)) and double-ionization (panel (b)) channel in collisions between O^{8+} and He atom at 1.44 MeV/amu projectile energy. Triangles: EE-CTMC, squares: NEE-CTMC.

single- and double-ionization cross section data of tables 1 and 2, respectively. Moreover, as a typical example, figure 3 shows the impact parameter dependence of the single- and double-ionization processes in collisions between O^{8+} and He atom at 1.44 MeV/amu projectile energy. While for the case of the single ionization the effective range of impact parameters is wider for the NEE-CTMC, for the case of double ionization the effective impact parameter range is wider for the EE-CTMC. For double ionization the spatial region is more confined for the NEE-CTMC.

For the ratio $R = \sigma^{++}/\sigma^+$, the CC method agrees quite well with the experimental results for all projectiles and impact energies. We can explain this behaviour with the properties of our basis set built up from CI wavefunction containing single- and double-ionized configurations for each channel. Our projection ensures that every channel has a contribution to both single and double ionization. If a favourable CI relation is found between single- and double-ionized configuration, the ionization ratio fits the experimental results independently of the number of the applied channels. The quality of results from the two different CTMC models are not unambiguous. The non-equivalent electron model gives better ratios for the lighter projectiles He^{2+} and Li^{3+} , however the equivalent electron model works better for the heavier projectiles, like C^{6+} and O^{8+} . This trend appears to have a simple explanation: for strong external fields,

Table 4. Total single-ionization cross sections for helium obtained in 1.44 MeV/amu. O^{q+} collisions, where q is the charge of the projectile. All cross sections are in units of 10^{-16} cm². The statistical errors of the CTMC calculations are less than 2%.

q	Z/v (amu)	Exp. value σ^+	EE-CTMC		
			NEE-CTMC	Garvey	CC
8	1.04	$6.7 \pm <8\%$	3.3	5.6	5.8
7	0.91	$5.5 \pm <8\%$	2.7	4.5	4.9
6	0.78	$4.2 \pm <8\%$	2.1	3.5	3.8
5	0.65	$3.5 \pm <8\%$	1.5	2.5	3.4
4	0.52	$2.51 \pm <5\%$	1.0	1.7	2.5

Table 5. Total double-ionization cross sections for helium obtained in 1.44 MeV/amu. O^{q+} -helium collisions, where q is the charge of the projectile. All cross sections are in units of 10^{-16} cm². CTMC errors are less than 7%.

q	Z/v (amu)	Exp. value σ^{++}	EE-CTMC		
			NEE-CTMC	Garvey	CC
8	1.04	$0.45 \pm <10\%$	0.775	1.01	0.32
7	0.91	$0.34 \pm <10\%$	0.54	0.85	0.28
6	0.78	$0.221 \pm <10\%$	0.35	0.565	0.18
5	0.65	$0.164 \pm <10\%$	0.20	0.41	0.12
4	0.52	$0.116 \pm <11\%$	0.05	0.12	0.10

Table 6. The ratio $R = \sigma^{++}/\sigma^+$ obtained from the cross sections of tables 4 and 5. All data should be multiplied by 10^{-3} , estimated experimental accuracy is 9%.

q	Z/v (amu)	Exp. value	EE-CTMC		
			NEE-CTMC	Garvey	CC
8	1.04	67	235	180	55
7	0.91	62	200	189	57
6	0.78	54	166	161	47
5	0.65	47	133	164	35
4	0.52	46	50	71	40

Table 7. Total cross sections and ratios for the 1.44 MeV/amu O^{q+} projectile ions obtained from EE-CTMC calculations. All cross sections are in units of 10^{-18} cm², ratios should be multiplied by 10^{-3} . The statistical errors of the calculation are less than 6%.

q	σ^+	σ^{++}	R
7	0.28	–	–
6	0.74	0.016	21.6
5	7.13	0.11	15.4
4	7.52	0.16	21.3

the difference between the single- and double-ionization thresholds of helium atom becomes less significant.

We now turn to projectiles which carry electrons into the collision. We use oxygen as projectile with an impact energy of 1.44 MeV/amu and charge states between $q = 7$ and $q = 4$. In the coupled-channel method we introduce the following time-dependent projectile–electron interaction:

$$V(\mathbf{r}, t) = -[(Z - 1)\Omega(r, t) + 1]/R(\mathbf{r}, t), \quad (21)$$

where the distance from the projectile is given by

$$R(\mathbf{r}, t) = ((x - b)^2 + y^2 + (z - v_p t)^2)^{1/2}. \quad (22)$$

The screening is treated as time dependent with $\Omega(r, t)$ (see equation (17)). Using energy minimization, Garvey *et al* [27] obtained the following parameters for O^{+q} $\{q = 7, 6, 5, 4\}$: $\{H = 1.36, 1.6467, 2.025, 2.5082,\}$ au and $\{d = 2.41, 2.6843, 3.0168, 3.4817\}$ au. Tables 4 and 5 present our results for single and double ionization, respectively. Our CC results agree well with experimental data for all projectile charge states. In contrast to bare projectiles the largest Sommerfeld parameter here is about unity, which means that even smaller number of collision channels (525) are sufficient to reach convergence. Similar to the previous cases, the equivalent electron CTMC model gives better results for single ionization than the non-equivalent one. For double ionization the ranking of the models is reversed. For the completeness, the double- to single-ionization ratios are also given in table 6. Except for the O^{4+} projectile charge state both CTMC results are a factor of three to four larger than the experimental data.

Projectiles carry electron(s) during the collisions can be ionized which can modify the single- and double-ionization cross sections. To check this contribution we present in table 7. The projectile single- and double-ionization cross sections using the EE-CTMC model. From the comparison between the data of table 7 and tables 4 and 5 one can see that the cross sections of single- and double-projectile ionization is negligibly small compared with the target ionization. These results verify that two-center effects do not give significant contributions to ionization in this energy region and our single-center coupled-channel method is appropriate.

There has been debate in the past about the importance of static and dynamic correlations in double ionization of He [29]. Our basis set includes static correlations directly. Dynamical correlation effects (i.e. the ionization of the second electron by the first ionized electron *via* the electron–electron repulsion [30]) are implicitly and only partially included in our CI basis expansion. The CTMC models ignore the dynamical correlation effects because the electron–electron interaction is neglected during the entire collision.

4. Summary and outlook

We have presented coupled-channel and CTMC calculations for single and double ionization of helium. We have investigated bare ions with charge from $Z = 2$ to $Z = 8$ in the 0.19–2.31 MeV/amu energy range. As a basis set in our CC calculations we used a configuration interaction wavefunction which was built up from Slater-like orbitals and Coulomb wave packets. We found that our results using the coupled-channel method are in very good agreement with the experiments even for large Sommerfeld parameters. A practical way to select the convergent basis was discussed. The CTMC calculations also describe the general trend of the experimental data correctly. However, the agreement between experiments and calculations are, in general, superior for the CC method. As an additional feature we performed calculations with partially stripped oxygen projectiles. In these cases the projectile–electron interaction was described by time-dependent particle model potentials. Our coupled-channel method again gives good agreement with experimental data.

We interpret the discrepancies between CC and CTMC calculations primarily as being due to the incomplete treatment of the electron–electron interaction within the classical simulations. Quantum effects appear to be less of a problem in the regime of the intermediate Sommerfeld parameter. Our results clearly show that neither the EE-CTMC nor the NEE-CTMC simulation can handle single and double ionization with the same accuracy.

Further work is in progress to test and compare our methods with experimental data for ionization of helium in negative boron, oxygen and fluorine ion collisions [31]. The aim of these studies is twofold. First we want to consider an improved inclusion of the electron–electron interaction in our CTMC method, and secondly we want to calculate angular differential ionization cross sections for ionization of helium in heavy particle collisions. To our knowledge there is no theoretical result available for angular differential ionization cross sections at intermediate energies using the coupled-channel method.

Acknowledgments

The work was supported by the Hungarian Scientific Research Found: OTKA Nos. T046095, T046454, the Tét Grant No. A-15/04, the grant ‘Bolyai’ from the Hungarian Academy of Sciences, ‘Stiftung Aktion Österreich-Ungarn’, No. 55ü1 and EU under contract no. HPRI-CT-2001-50036.

References

- [1] Knudsen H, Andersen L A, P Hvelplund C, Astner C, Cederquist H, Danared H, Liljeby L and Renfelt K-G 1984 *J. Phys. B: At. Mol. Phys.* **17** 3545
- [2] Shah M B and Gilbody H B 1985 *J. Phys. B: At. Mol. Phys.* **18** 899
- [3] Ullrich J, Moshhammer R, Dörner R, Jagutzki O, Mergel V, Schmidt-Böcking H and Spielberg L 1997 *J. Phys. B: At. Mol. Opt. Phys.* **30** 2917
- [4] Ford A L and Reading J F 1994 *J. Phys. B: At. Mol. Opt. Phys.* **27** 4215
- [5] Luedde H J, Kirchner T and Horbatsch M Quantum mechanical treatment of ion collisions with many-electron atoms *Photonic, Electronic, and Atomic Collisions* ed J Burgdörfer *et al* (Princeton, NJ: Rinton) p 708
- [6] Keim M, Achenbach A, Lüdde H J and Dreizler R M 2003 *Phys. Rev. A* **67** 062711
- [7] Wherman L A, Ford A L and Reading J F 1996 *J. Phys. B: At. Mol. Opt. Phys.* **29** 5831
- [8] Díaz C, Martín F and Salin A 2002 *J. Phys. B: At. Mol. Opt. Phys.* **35** 2555
- [9] Tushima W 2001 *Phys. Rev. A* **64** 024701
- [10] Schulz D R and Krstic P S 2003 *Phys. Rev. A* **67** 022712
- [11] Sahoo S, Mukherjee S C and Walters H R J 2004 *J. Phys. B: At. Mol. Opt. Phys.* **37** 3227
- [12] Martín F 1999 *J. Phys. B: At. Mol. Opt. Phys.* **32** R197
- [13] Pfeiffer C, Grün N and Scheid W 1999 *J. Phys. B: At. Mol. Opt. Phys.* **32** 53
- [14] Barna I F, Grün N and Scheid W 2003 *Eur. Phys. J. D* **25** 239
- [15] Barna I F and Rost J M 2003 *Eur. Phys. J. D* **27** 287
- [16] Barna I F 2004 *Eur. Phys. J. D* **30** 5
- [17] Tókési K and Hock G 1996 *J. Phys. B: At. Mol. Opt. Phys.* **29** L119
- [18] Abrines R and Percival I C 1966 *Proc. Phys. Soc. (London)* **88** 861
- [19] Olson R E and Salop A 1977 *Phys. Rev. A* **16** 531
- [20] Tókési K and Hock G 1994 *Nucl. Instrum. Methods B* **86** 201
- [21] Tókési K and Kövér Á 2000 *J. Phys. B: At. Mol. Opt. Phys.* **33** 3067
- [22] Barna I F 2002 Ionization of helium in relativistic heavy-ion collisions *Doctoral Thesis* University Giessen Giessener Elektronische Bibliothek <http://geb.uni-giessen.de/geb/volltexte/2003/1036>
- [23] Ho Y K 1986 *Phys. Rev. A* **34** 4402
- [24] Cowan R D 1981 *The Theory of Atomic Structure and Spectra* (Chicago, IL: University of California Press)
- [25] McKenzie M L and Olson R E 1987 *Phys. Rev. A* **35** 2863
- [26] Green A E S 1973 *Adv. Quantum Chem.* **7** 221
- [27] Garvey R H, Jackman C H and Green A E S 1975 *Phys. Rev. A* **12** 1144
- [28] Reinhold C O and Falcón C A 1986 *Phys. Rev. A* **33** 3859
- [29] McGuire J H 1997 *Electron Correlation Dynamics in Atomic Collisions* (Cambridge: Cambridge University Press) p 124
- [30] Pattard T and Burgdörfer J 2001 *Phys. Rev. A* **64** 042720
- [31] Zappa F, de Barros A L F, Coelho L F S, Jalbert Ginette, Magalhaes S D and de Castro Faria N V 2004 *Phys. Rev. A* **70** 034701